

## Wellbore Instability Analysis to Determine the Failure Criteria for Deep Well/H Oilfield

Muayad K. Bandara, Nagham J. Al-Ameri\*

*Petroleum Engineering Department, Collage of Engineering, University of Baghdad, Baghdad, Iraq*

Received September 17, 2023; Accepted January 17, 2024

### Abstract

Wellbore failure criteria are essential issues during drilling deep wells. When drilling activities begin, the major stresses will change, and a new set of forces will be created in the rocks that surround the borehole. These stresses will be caused by the drilling operations themselves. This study concern with estimating stress state and magnitude around the wellbore by constructing a one-dimensional mechanical earth model (1D-MEM) that will help to predict failure criteria during deep wells drilling. A set of well logs data measurement has been used to compute failure criteria parameters for nine formations along the studied well. Repeated formation pressure and laboratory core testing are used to validate the calculated results of 1-D MEM. The prediction of failure criteria along the nine studied formations shows that for Ahmadi, Nahr Umr, Shuaiba, and Zubair formations, the wellbore failure criteria appear unsafe compared to other formations. The results of stress analyses indicate that the breakout factors wasn't affected by wellbore azimuth because of low-stress contrast along the these formations. Furthermore, shear failure can be prevented by drilling the well with an inclination of less than 35°. As well as, to prevent breakdown the well should be drilled with an inclination between 25° to 65° in the direction of minimum horizontal stress. These important results could be used to pridict accurate wellbore trajectory when planning to drill nearby wells in the future.

**Keywords:** *Elastic properties; Failure criteria; Geomechanical properties; Wellbore stress; Stress direction.*

## 1. Introduction

Wellbore failure criteria analysis is the most challenging problem in terms of cost and time in deep drilling operations. Many theoretical models [1] are proposed to analysis the failure caused by mechanical instability of the wellbore to predict hole washout as well as tensile failure (fracking) and find the right pressure from the used mud to keep the borehole from failing. He illustrated that the model can be employed in vertical and deviated wells in a region having both normal and in-situ stresses. His findings demonstrate the effect of the wellbore angle on the failure of the wellbore and the correct selection of mud weight windows. Two distinct stress models are presented [2] which are the elastic model and the failure model (poro-elastic model). The analysis revealed that the proposed failure model appears to be more accurate for shale than elastic models. Seven different criteria of failure [3] are proposed and compared them to release polyaxial data ( $\sigma_1 > \sigma_2 > \sigma_3$ ) for five various types of rock with different states of stress. They used a new grid search algorithm to select the most appropriate parameters that describe each failure criterion and the misfits of the data that go with it. Overall, they discovered that the majority of the test data fit perfectly to the polyaxial criteria of Modified Wiebols and Cook, as well as Modified Lade. A new model known as the Mogi-Coulomb model [4], which allows them to quickly determine the critical mud drilling window They also stated that Mohr-Coulomb is typically used for brittle rock; however, this criterion includes maximum and minimum stresses and does not consider intermediate stresses. Go-

mechanical model [5] were used to evaluate the prearranged wellbore locations for the development of an offshore oilfield in Australia. The findings of the research demonstrated that natural fractures of any size could have a big impact on the condition of in-situ stresses and stresses that were caused by revealing the borehole annulus. used Different failure criteria were used for an appropriate selection of mud weight [6] to prevent the wellbore from becoming unstable. They decided to go with the Mohr-coulomb, Mogi-coulomb, and Hoek-Brown combinations. In addition to this, they discovered that the Mohr-Coulomb model was conservative in its predictions, whereas the Mogi-Coulomb model provided them with desirable outcomes in comparison to the Hoek-Brown model. A comparison of thirteen regularly used failure criteria are good [7] estimation and identified the differences and similarities that existed between them. According to the findings, some of them may be utilized to determine the higher boundaries of the minimum mud weight (Tresca, Von Mises, and Inscribed Drucker-Prager), while other ones can be utilized to determine the lower limits of the minimum mud weight (Drucker-Prager). Finally, the outcomes of the cases that were studied appear to be the same for the Modified Wiebols-Cook, Modify-Lade, and Mogi-coulomb models. The in-situ and induced stresses can be estimated by developing a fully MEM [8], Their research aimed to predict the stability of the wellbore and the pressure at which breakout occurs in both vertical and inclined wells. The model was constructed for a formation in the southwest of Iran using a wide variety of petrophysical techniques, field data, and laboratory testing. Predictions of the breakout pressure were made using the Mohr-Coulomb, Hoek-Brown, and Mogi-Coulomb failure criteria. They found that the Hoek-Brown criteria provided the most accurate results. The authors came to the conclusion that an overall increase in wellbore slope produces an increase in breakout pressure as a result of the sensitivity analysis that was done for the angle of inclination and the azimuth. This problem has been discussed in this study for one of the enormous mature oilfields of the Iraqi fields which is the H oilfield. H oilfield is measures around 38 km in length and 12 km in width, most of those areas are desert and are flat.

H field was discovered in 1976, eight wells were drilled and seven oil-bearing formations were discovered. The structure was defined by 2D seismic data shot. Up to June 2010, eight wells were the deepest well, where it reached a depth of 4,788m down to the Lower Cretaceous Sulaiy formation. The seven oil-bearing formations of the H oilfield are Tertiary Jeribe and Upper Kirkuk; Upper Cretaceous Hartha; Tanuma; Khasib; Mishrif; Nahr Umr; and Lower Cretaceous Yamama.

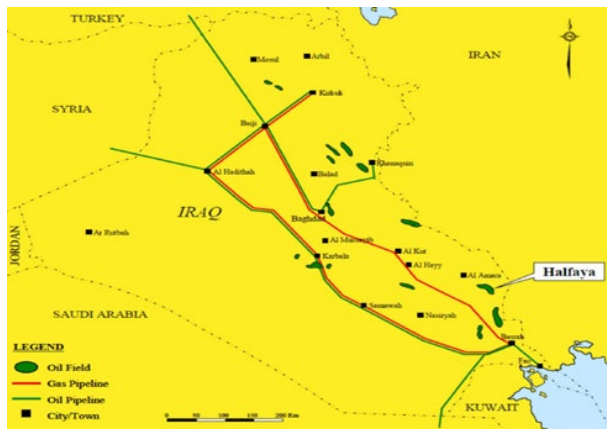
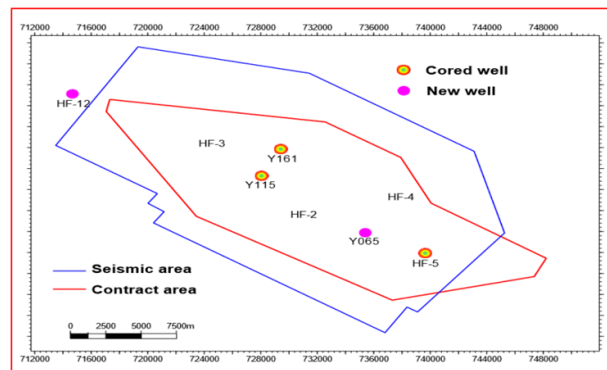


Fig. 1. Location of H oilfield (modified after [9]).



2. Locations of drilled wells in Yamama formation Fig. (modified after [10]).

H oilfield is located on the Arabian Shelf, which is adjacent to the Zagros tectonic zone. The structure of the anticline is a low-dip anticline in which the long axis is nearly perpendicular to the Zagros. There is no large fault that could be recognized by seismic data from the region. According to its structure, failure criteria are essential to be recognized during good planning. The geologic column for the H oilfield is viewed in Fig.3.

Formation	Lithology	Top Depth (m)	Height (m)	Lithology description
Upper Fars		10	1310	Mudstone and sandstone, gypsum mudstone at the bottom
Lower Fars		1320	590	Sandstone, mudstone, limestone, gypsum, salt rock interbedding
Jeribe -Euphrates		1910	30	Dolomite, gypsum
Kirkuk		1940	436	Sandstone, sandy dolomite, marlite interbedding
Jaddala/Aaliji		2376	134	Chert limestone, marlite and shale
Shiranish/Hartha		2510	116	Limestone, marlite at the bottom
Sadi/Tanuma		2626	134	Marlite at the top, limestone and shale
Khasib		2760	70	Mainly marl
Mishrif A		2830	410	Limestone with shale and marlite
Mishrif B	Limestone with Chert			
Rumaila/Ahmadi		3240	50	Limestone
Mauddad		3290	170	Limestone
Nahr Umr		3460	250	Shale, unconsolidated sandstone and shale
Shuaiba		3710	200	Limestone with shale
Zubair/Ratawi		3910	360	Sandstone, mudstone with shale
Yamama		4100	250	Limestone
Sulaily		4350		Limestone

Fig. 3. Stratigraphy column for H oilfield (modified after [10]).

## 2. Materials and methods

### 2.1. Mechanical earth modeling (MEM)

The mechanical model was used to create a constructive geomechanical model that predicted pore pressure and far-field stresses as a function of depth. Elastic rock parameters such as Poisson's ratio, shear modulus, bulk modulus, and Young's modulus and strength were also calculated.

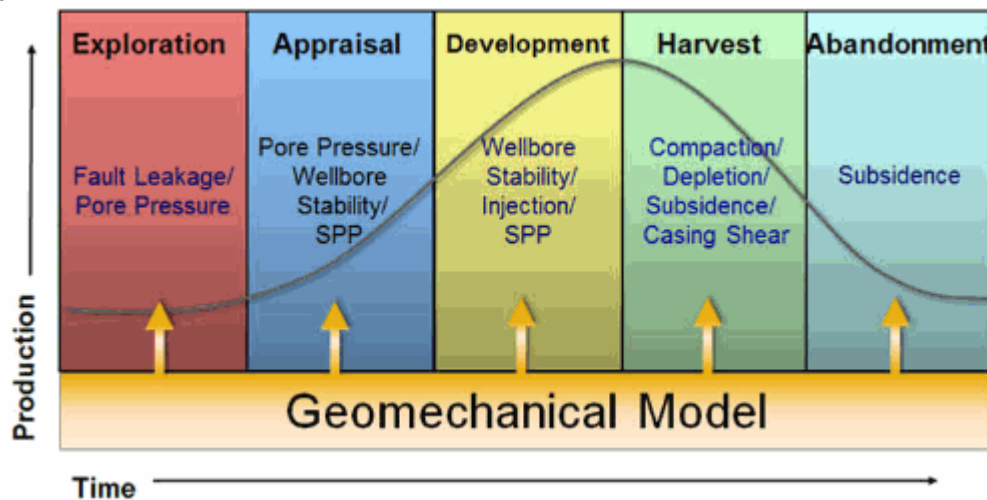


Fig. 4. The workflow for the study's methodology.

Friction angle, rock cohesiveness, tensile strength, and unconfined compressive strength are all rock characteristics by input the data as presented in Fig. 4. The first step was collecting the required data to create the model (such as well as logs including density, gamma ray, shear wave velocities, compression wave velocities, caliper, bit size), and measured data (such as Laboratory core testing confirmed its authenticity). Then the profiles for the 1D- MEM constituents can be constructed. The mechanical earth model consists primarily of vertical stress, pore pressure, the elasticity and strength of the rock, and horizontal stresses. Validation can be done using the observed data from repeated formation test (RFT), and core rock mechanical laboratory test [11].

### 2.1.1. Vertical stress

Vertical stress, also known as overburden stress ( $S_v$ ), is the pressure put on a point by the weight of formations that are below it and contain fluid. One of the principal strains is vertical stress, which points in the direction of the earth's core. The depth-dependent propagation of overburden pressure results in an increase in sediments [12]. The vertical stress was calculated by incorporating the derived densities from of Bulk Density log that covered the rocks from Mishrif formation to Yamama formation, by using equation (1) [13-15].

$$SV = g \int_0^z \rho b(z) dz \tag{1}$$

where  $\rho b(z)$  represent bulk density of formation depending on the depth and can be obtained from the density log;  $Z$  represents depth. While the missing density at the surface interval is extrapolated by using equation (2) [16].

$$\rho M = \rho_{mudline} + A_o \times (TVD - Air\ gap - Water\ depth)^\alpha \tag{2}$$

where  $\rho M$  is the density at ground level in  $gm/cm^3$ ;  $\rho_{mudline}$ : density of substance at ground level (soil density  $1.65 gm/cm^3$ ); air gap: height of rotary table from the ground (m); TVD: the true vertical depth (m);  $A_o$  and  $\alpha$ : Equation constants.

The vertical stress profile is shown in the third track of Fig. 5 for the studied formations.

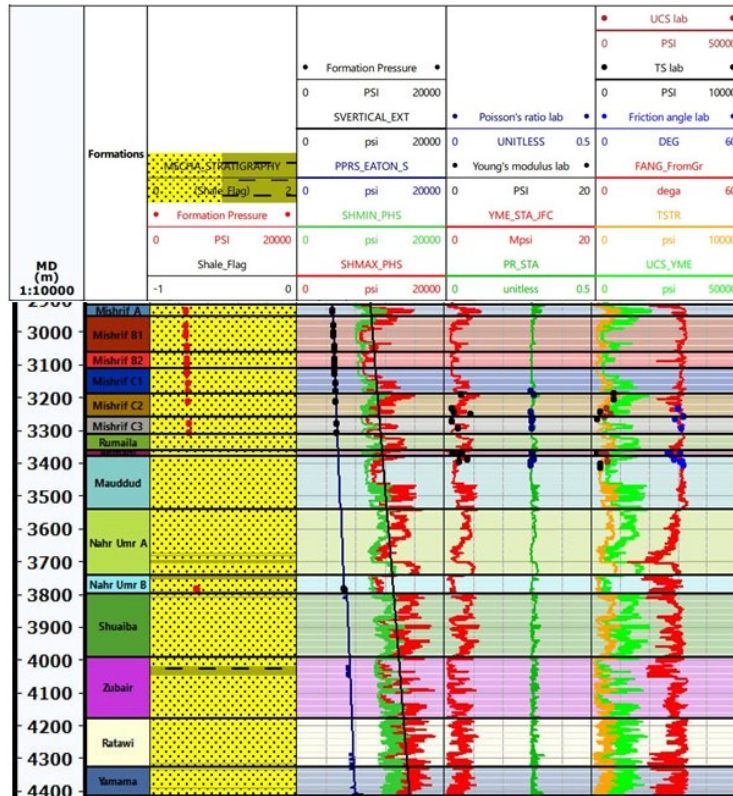


Fig. 5. Components of 1-D-MEM results.

### 2.1.2. Shale flag (mechanical stratigraphy)

The profile of shale flag was calibrated with pore pressure taken from permeable layers by using RFT technique of formation test (blue circle in third track) and show good agreement as illustrated in as illustrated in the second track of Fig. 5 under the name of shale flag. The inconsistency of the pressure scale arises from the significant disparity between the upper scale value of 20,000 psi and the desired value of 10,000 psi, which is half of the current upper limit. This adjustment is necessary in order to properly assess the sensitivity of pressure changes, as demonstrated in the second track of Fig. 5 under the name formation pressure for the studied formations.

### 2.1.3. Formation pressure

Pore pressure is a crucial factor in drilling plane, petroleum production, and geomechanical modeling. It significantly affects both the wellbore's deformation and the stability analysis of the drill hole. Pore pressure is estimated by direct and indirect methods. The direct methods and pore pressure were measured by some techniques such as RFT and DST.

In the indirect method, the profile of pore pressure was calculated by merging the normal pressure and geo-pressure profiles. The profile of the hydrostatic pressure ( $P_h$ ) was calculated by using equation (3) and the profile of geo-pressure in this study was calculated according to equation (4), using the Eaton method [17]. This equation was used to estimate the pore pressure in the shale's formations (nonproducing zone). On the other hand, the linear interpolation method was used to predict the pore pressure in permeable limestone (production section) as demonstrated in the third track of Fig. 5 under the name PPRS EATON S. The resultant profile was calibrated against actual pressure point measurements from indirect methods to minimize the uncertainty of the estimated pore pressure) as demonstrated in the third track of Fig. 5 under the name formation pressure for the studied formations.

$$P_{hydrostatic} = \int_0^z \rho_w g dz \quad (3)$$

$$P_p = \sigma_v - (\sigma_v - P_{pnorm}) * a * \left(\frac{\Delta t_{norm}}{\Delta t}\right)^n \quad (4)$$

### 2.1.4. Mechanical properties

Rock mechanical properties are mostly related to subsidence issues such as sand production, wellbore instability, and fracturing operations. The elastic properties including Young's modulus (E) (resistance of rock sample to uniaxial stress), Poisson's ratio( $\nu$ ) (measuring the rock expands with respect to a shorting in axial), the Shear modulus (G)(the amount of rock misshapes in response to shear stress) and the Bulk modulus(K) (the hardness under volumetric compression). The strength properties including internal friction angle( $\phi$ ) (estimation of rock failure), Cohesive Strength( $S_o$ )(defines a reflectance to the degree of adherence between connected molecules), Tensile strength( $T_s$ ) (the rock resistance), Unconfined compressive strength (UCS) (the highest axial compressive stress in a triaxial test that a rock withstands before failing) [12]. These properties are considered essential components in the determination of the magnitude of horizontal stresses, analysis of the stability of the wellbore, and prediction of stable mud windows to achieve stable drilling.

These properties are estimated by the direct laboratory methods and indirect petrophysical methods, usually direct methods are used to calibrate the estimated profiles of the property's estimation from indirect methods. In this study, the mechanical properties of rock were estimated from indirect petrophysical methods using three types of logs (shear and slowness velocities, bulk density) as expressed in equations 5 and 6 which were used to calculate the shear and bulk moduli (G and K). Shear moduli is the measurement of the stiffness of material resistance against the applied shear stress. Bulk moduli (K) measures the capability of the material to resist the change in volume when all sides of the material are under compression [17]. Hence, from the two moduli (shear and bulk) the dynamic profiles of Young's modulus(E) in Mpsi and Poisson ratio( $\nu$ ) can be estimated, by using the equations 7 and 8 sequentially.

$$G_{dyn} = 13474.45 * \frac{\rho b}{(\Delta t_{shear})^2} \quad (5)$$

$$K_{dyn} = 13474.45 * \left[ \frac{\rho b}{(\Delta t_{comp})^2} \right] - \frac{3}{4} * G_{dyn} \quad (6)$$

where:  $\rho b$  is bulk density of the formation ( $\text{g/cm}^3$ );  $(\Delta t_{shear})$  and  $(\Delta t_{comp})$  are acoustic travel time of shear and compressional in  $\mu\text{sec/ft}$ .

$$E_{dyn} = \frac{9 * G_{dyn} * K_{dyn}}{G_{dyn} + 3 * K_{dyn}} \quad (7)$$

$$v_{dyn} = \frac{3K_{dyn} - 2G_{dyn}}{6K_{dyn} + 2G_{dyn}} \quad (8)$$

These dynamic rock parameters are converted into static rock properties via accessible efficient correlations. Because of the low constraint of the logging device and the effects of pore pressure, stress, strain, and cementation dynamic rock values are frequently larger than static rock properties. The estimation of static profiles shows a good matching with the direct measurements from laboratory testing, as demonstrated in the fourth track of Fig. 5 for the studied formations.

Many correlations exist to convert dynamic Young's moduli to static Young moduli, such as the Plumb Bradford, Modified Morales, Morales, and John Fuller correlations. The most accurate and appropriate correlation was the John Fuller correlation, which was applied to sandstone and shale formations and used to estimate the static Young's modulus profile [18].

### 2.1.5. Horizontal stress magnitudes and directions

A rock creates horizontal movement when vertical stress is applied perpendicularly, which have the same value but only vertical pressure is present. While tectonic activities and faulting influences horizontal stresses. In tectonic activity, such as isotropic formation, only vertical stress occurs if the magnitudes of the minimum and maximum horizontal stresses are identical. Horizontal stresses have variable values and should be considered if there is tectonic activity and a significant fault [19]. When there are no tectonic activities the minimum and maximum stresses have existed, there are different values for both minimum and maximum stresses.

Poro-elastic model assuming a poro-elastic flat-layer distortion of the rock formation and coupling with specific consistent strains,  $\epsilon_{SHMIN}$  and  $\epsilon_{SHMAX}$  will be act on formation in orientation of mini- and maxi- horizontal stresses, respectively, as demonstrated in the third track of Fig. 5. The model equations are mainly based on the Young module, pore pressure, density, and rock deformation as expressed in the equations 9 and 10.

$$\sigma_h = \frac{v}{1-v} * \sigma_v - \frac{v}{1-v} * \alpha P_o + \alpha P_o \frac{s * v}{1-v} * \epsilon_h + \frac{v * E}{1-(v)^2} * \epsilon_H \quad (9)$$

$$\sigma_H = \frac{v}{1-v} * \sigma_v - \frac{v}{1-v} * \alpha P_o + \alpha P_o \frac{s * v}{1-v} * \epsilon_H + \frac{v * E}{1-(v)^2} * \epsilon_h \quad (10)$$

where  $\sigma_H$  and  $\sigma_h$  are the maximum and minimum horizontal stresses respectively;  $v$  refers to Poisson's ratio;  $\sigma_v$  represents the vertical stress;  $\alpha$  indicates Biot's coefficient (conventionally  $\alpha=1$ );  $E$  represents the static Young's modulus;  $P_p$  represents the pore pressure;  $\epsilon_h$  and  $\epsilon_H$  are the strain in the direction of  $\sigma_h$  and  $\sigma_H$ , respectively, as expressed in equations 11 and 12.

$$\epsilon_h = \frac{\sigma_v * v}{E} * \left( 1 - \frac{v^2}{1-v} \right) \quad (11)$$

$$\epsilon_H = \frac{\sigma_v * v}{E} * \left( \frac{v^2}{1-v} - 1 \right) \quad (12)$$

### 2.1.6. Direction of horizontal stresses

Another crucial role of reservoir geomechanics is the estimation of horizontal stress orientation. It is playing a significant part in drilling by setting a wellbore trajectory that is optimum, and it also aids in production by locating the preferred perforation orientation and preventing sand generation. There are numerous logging tools available, including resistivity and cross-

dipole logs, caliper logs, ultrasonic borehole viewers, and formation micro imagers (FMI). When stress concentration around a borehole exceeds the capacity of the rock, caving or breakouts are likely to result [20].

In vertical wellbores, breakouts occur in a direction perpendicular to the maximum horizontal stress and parallel to the minimum horizontal stress. While in deviated wells, the breakout development was influenced by the wellbore, orientations, and magnitudes of stresses as well as the wellbore trajectory [21].

## 2.2. Around wellbore failure criteria analysis

Failure criteria chose the safe mud weight window by comparing wellbore stresses to rock strength, so preventing the most common instability problems shear failure and tensile failures from occurring. Consequently, a number of failure criteria have been developed for borehole stability analysis that rely on the intermediate principal stress  $\sigma_2$ . These criteria are divided into two groups: independent failure criteria (which ignore intermediate stress) like Mohr-Coulomb and dependent failure criteria (which take internal stress into account) like Modified Lade and Mogi-Coulomb failure criteria.

Borehole collapse occurs when the compressive strength of the rock-applied stress is larger than the stress applied by drilling mud, or Hole enlargement occurs when the pressure of drilling fluid is lower than formation pressure. Breakout failure is the term used to describe various failure types. The signs of that are poor cementing, inflexible formation fluid, ineffective hole cleaning that necessitates a rise in hydraulic needs, and challenges with the performance and response of well log tooling. Instability of the well occurs when the pieces of rock collapse fall down into the hole and settle on the drill string causing the inability to withdraw the drill string which causes a stuck pipe [22-23].

Narrowing or hole closure results from the creep under the influence of the overburden (plastic flow of the rock), which usually occurs in sandstone, shale, and salt sections. The symptoms include difficult casing landing, increased torque, possible pipe sticking, and preventing hole closer requirement to repeat reaming operations.

Fracturing occurs when the pressure of mud weight exceeds the pressure of formation fracture. The signs of that are lost circulation and well control issues (kick and blowout), which arise when drilling fluid invades the formation and decreases the influence of the drilling fluid pressure that has been applied.

## 2.3. Failure analysis

Failure criteria is one of the important results of wellbore stability analysis, which consists of four critical values. These critical values are defined with respect to the mud pressure [20] as clarified in Fig. 6, which is pressure equivalent to drilling mud weight:

1. Pore pressure ( $P_p$ ): As shown the mud weight below the pore pressure may result in a kick and/or washout (wellbore collapse).
2. Shear failure pressure (PBKO): A breakout may occur if the mud weights decrease below the PBKO limit.
3. Formation breakdown pressure (FP): Also known as breakdown pressure, or fracture pressure [12], this pressure is required to cause rock fracture at a depth. The fracture pressure may be less than the minimum horizontal stress if the rocks already have pre-existing flaws. The maximum fracture pressure for unaffected rocks will occur following the initiation of a tensile failure and the occurrence of mud loss. When the tensile strength and the least hoop stress are equivalent, the fracture pressure can then be determined using Kirsch's solution.
4. Minimum horizontal stress ( $h$ ): Mud pressures higher than the minimum horizontal stress reopen fissures in the wellbore wall and result in mud loss [5].

In conclusion, it is for investigation of a stable wellbore the safe mud weight generally should be designed to be greater than the shear failure pressure and the pore pressure and less than the formation breakdown pressure and the minimum horizontal stress. Otherwise, an

unstable wellbore will be produced with so much rock material failing from the borehole circumference. Then, due to the excessive total volume of failed rock material and drilled cuttings and inadequate lifting capacity caused by annulus enlargement, a borehole pack-off can occur on the bottom hole assembly. Hence, this circumstance is sometimes called wellbore collapse because it seems that the wellbore collapsed in the drilling, and the cutting cannot be circulated out of the hole.

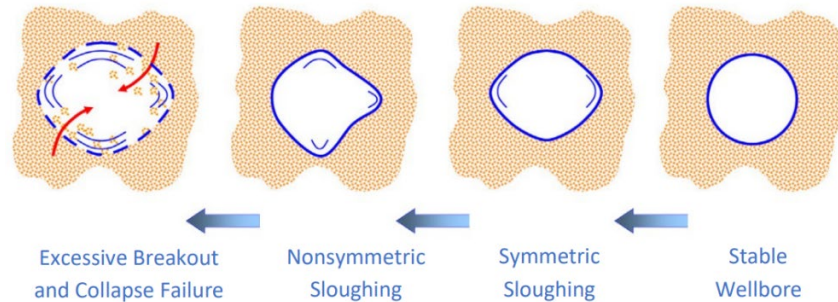


Fig. 6. The concept of shear failure around the wellbore (modified after [12]).

### 3. Results and discussion

#### 3.1. Wellbore failure

After the complete construction of 1D-MEM, it must be validated before its application by performing a failure under actual failure conditions of the wellbore which is executed by using the image formation test, caliper logs, and the drilling events. The failure criterion which investigates greater match is considered the most practical criterion for interval interest. In this study three failure criteria are applied for a geomechanical model such as Mohr-Coulomb illustrated in Fig. 7, modified-Lade illustrated in Fig. 8, and Mogi-Coulomb illustrated in Fig. 9, to foresee the unstable regions in the wellbore.

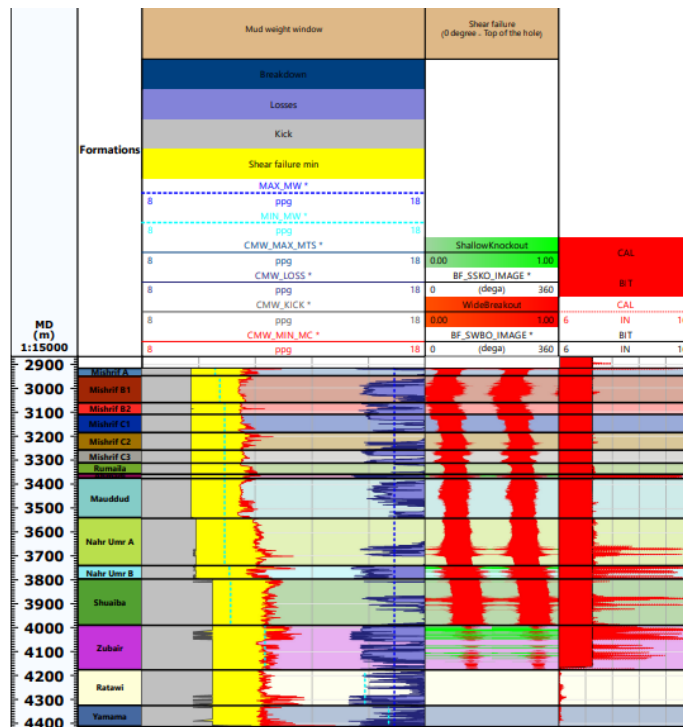


Fig. 7. Breakout force using Mohr-Coulomb criterion.

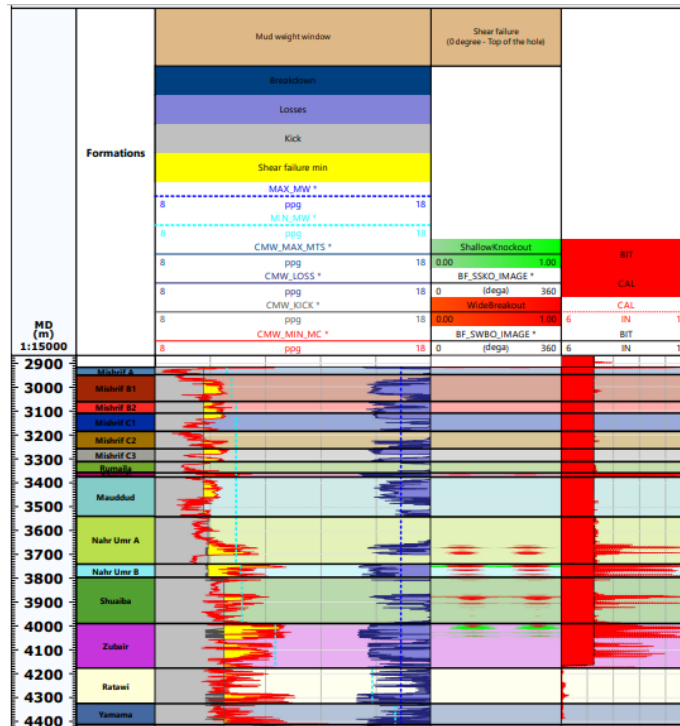


Fig. 8. Breakout force using Modified-Lade criterion.

From the obtained results, the Mohr-Coulomb criteria appeared overstate while the Modified-Lade criteria was conservative in foreseeing rock failure but the Mogi-Coulomb criterion showed a more reasonable and appropriate in foreseeing rock failure for H oilfield and showed a good agreement with the observed breakouts from logs because Mogi-Coulomb take intermediate principal stress in consideration when analysis the failure, as demonstrated in the third and fourth track of Fig. 9.

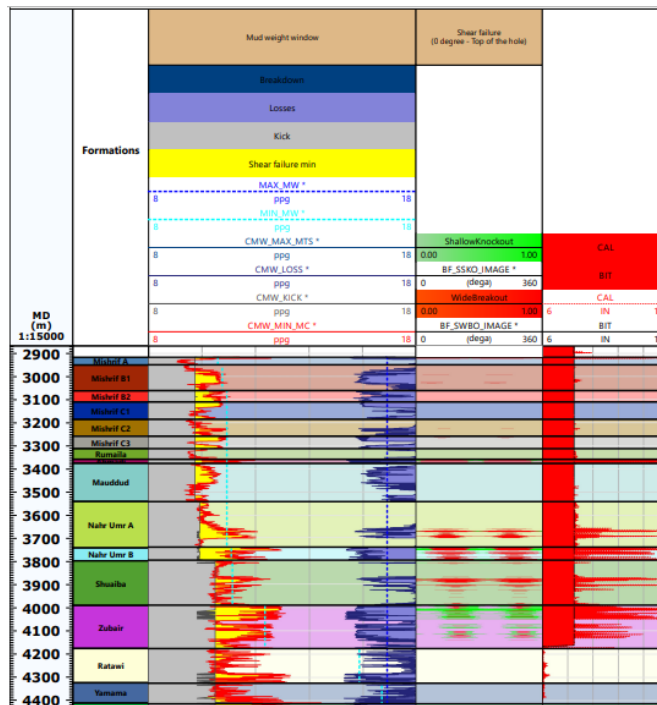


Fig. 9. Breakout force using Mogi-Coulomb criterion.

### 3.2. Single depth sensitivity analysis for the studied formations

In order to predict the optimum mud weight for planned wellbore trajectories, a single depth sensitivity analysis was carried out after the completion and validation of 1D MEM, which included rock properties, pore pressure, and in-situ stresses (vertical stress and horizontal stresses). The results of the sensitivity analysis are shown in two plots: stereonet plots and line plots, which make use of the current wellbore trajectory, current mud weight, and MEM outputs such as pore pressure, in-situ stresses, and rock elastic and strength properties for a certain depth. Shear failure and breakdown failure are examples of stereonet plots. The stereonet plot has circles in the center that represent the well's inclination, which ranges from zero at the center to 90° on the outside circle, and circles in the middle that represent the well's azimuth, which ranges from zero at the top to 360° in a clockwise direction. The color shading on the graph indicates the quantity of mud needed to prevent failures, as shown in Fig.10-a and b.

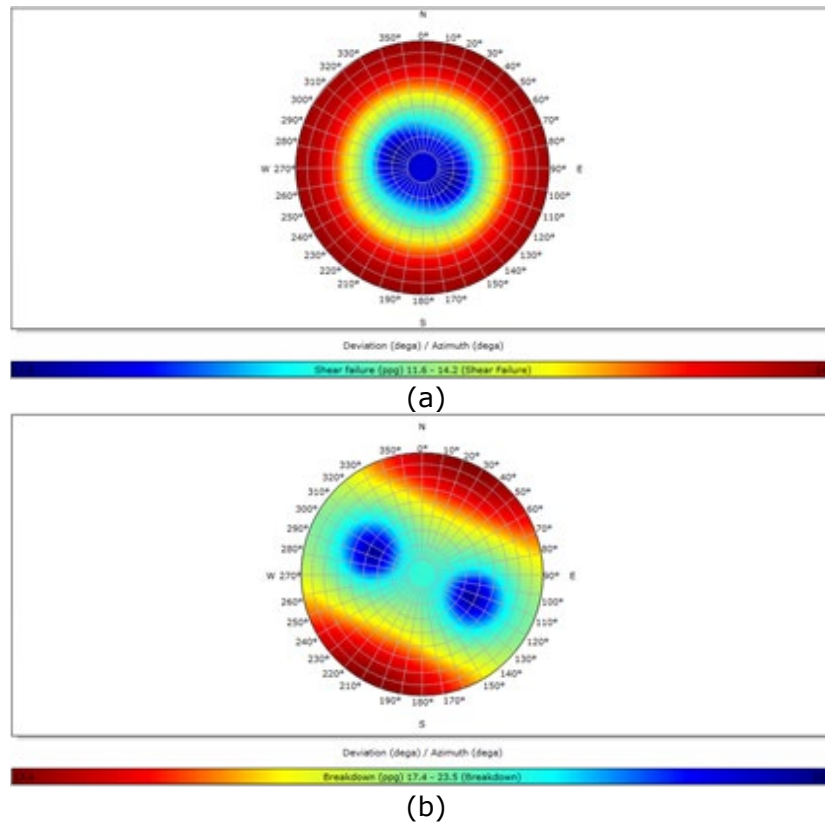


Fig. 10. Plots of mini-mud weight by using Mogi-Coulomb failure criterion: (a) breakout mud weight vs. orientation, (b) breakdown mud weight vs. orientation.

In breakouts stereonet plots, as shown in Fig 10-a, the blue color indicates the least amount of mud weight that can be used without any potential shear failure, and the red color indicates the highest amount of mud that causes tensile failure. Similarly, in breakdown failure stereonet plots, as shown in figure Fig.10-b, the blue color indicates the least amount of mud weight that can be used without any potential tensile failure. Mud weight sensitivity for borehole trajectory is the second part of sensitivity analysis. The safe mud weight window at a particular azimuth may be found by plotting the mud weight window against the borehole inclination, as illustrated in Figure Fig.10-c. On the other hand, as seen in Fig.10-d, the diagram of the mud weight window versus borehole azimuth shows the safe mud weight window as a function of azimuth at a particular deviation. Drilling data studies and previously built geomechanical modeling were used to determine the drilling fluid density window. Using the Mogi-Coulomb criterion for the MEM, which was constructed as shown in Figure 10, the stereographic plots have been utilized to estimate safe mud weight in relation to orientation and inclination

and to expect the impact of azimuth and deviation on breakout and breakdown of the rock. This sensitive single-depth study was carried out at essential depths throughout troublesome formations, including shale and weak sandstone for the dangerous layers of the H-oil field.

**3.2.1. Single depth sensitivity analysis for Ahmadi formation**

The single depths sensitivity analysis was applied in this formation according to failure which was predicted by the Mogi-Coulomb criterion with actual mud weight.

Stereonet plots for depth (3362.9) m showed the breakouts with inclination (0-40) degree is most save and stable regarding shear failure, even when using low mud weight in directions of minimum horizontal stress, but for inclinations 60 degrees and above, shear failure occurs even with a high mud weight in both directions of minimum and maximum horizontal stress, and stereonet plots for breakdown show that tensile failure most likely occurs with inclination 80 and above towards of maximum horizontal stress. While in the direction of minimum horizontal stress, breakdown may not occur even with high mud weight, as illustrated in Fig. 10-a and b.

**3.2.2. Single depth sensitivity analysis for Nahr Umr formation**

Stereonet plots for depths (3669) m, showed the breakouts with inclination (0-45) degree is the most save and stable regarding shear failure, even when using low mud weight in directions of minimum horizontal stress, for inclinations 60 degrees and above, the shear failure occurs even using high mud weight in both directions of minimum and maximum horizontal stress. Stereonet plots for breakdown show that tensile failure most likely occurs with an inclination of 80 degrees and above, towards maximum horizontal stress, and requires low drilling mud weight to maintain the wellbore stabilized. While in the direction of minimum horizontal stress, breakdown may not occur even with high mud weight, Fig.11-a and b.

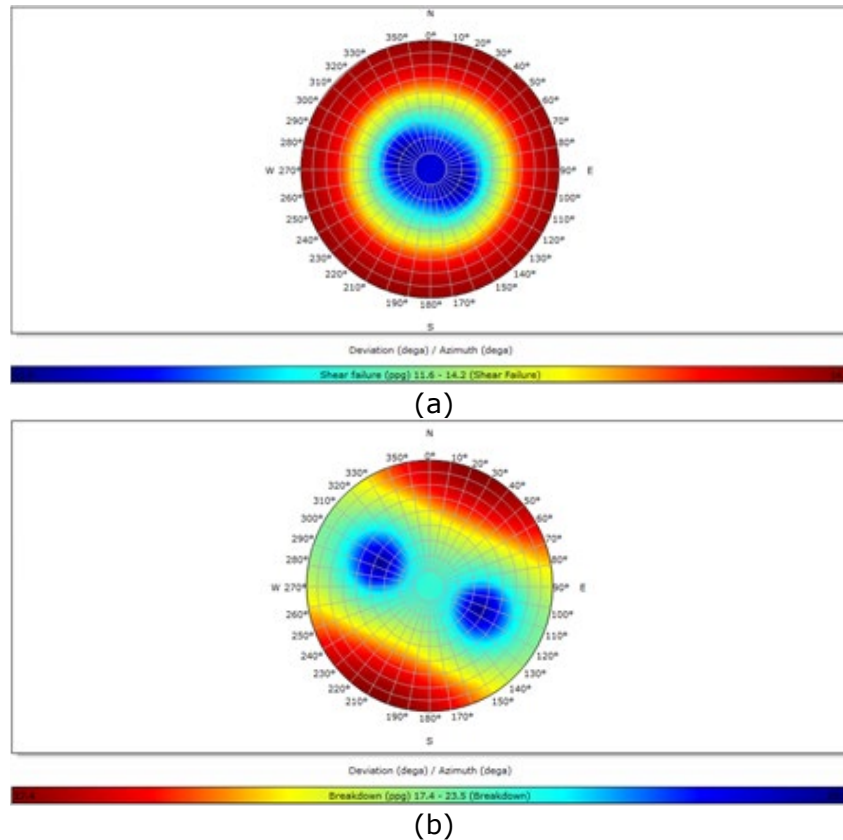


Fig. 11. Plots of mini-mud weight by using Mogi-Coulomb failure criterion: (a) breakout mud weight vs. orientation, (b) breakdown mud weight vs. orientation.

### 3.2.3. Single depth sensitivity analysis for Shuaiba formation

Stereonet plots for depths (3878.8) m, showed the breakouts with inclination (0-45) degree is the most save and stable regarding shear failure, even when using low mud weight in directions of minimum horizontal stress, for inclinations 60 degrees and above, the shear failure occurs even using high mud weight in both directions of minimum and maximum horizontal stress. Stereonet plots for breakdown show that tensile failure most likely occurs with an inclination of 90 degrees and above, towards maximum horizontal stress, and requires low drilling mud weight to maintain the wellbore stabilized. While in the direction of minimum horizontal stress, breakdown may not occur even with high mud weight, Fig.12-a and b.

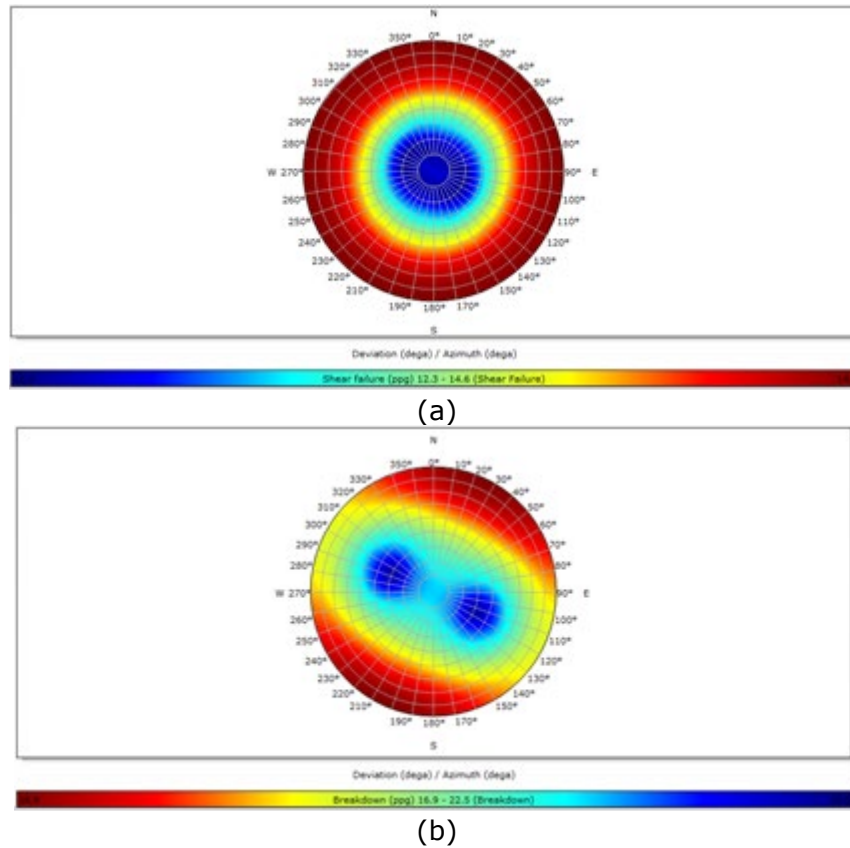


Fig. 12. Plots of mini-mud weight by using Mogi-Coulomb failure criterion: (a) breakout mud weight vs. orientation, (b) breakdown mud weight vs. orientation.

### 3.2.4. Single depth sensitivity analysis for Zubair formation

Stereonet plots for depths 4011 m showed the breakouts with inclination (0-45) are the most save and stable regarding shear failure, even when using low mud weight in directions of minimum horizontal stress, for inclinations 60 degrees and above, the shear failure occurs even using high mud weight in both directions of minimum and maximum horizontal stress. Stereonet plots for breakdown show that tensile failure most likely occurs with an inclination of 60 degrees and above, towards maximum horizontal stress, and requires low drilling mud weight to maintain the wellbore stabilized. While in the direction of minimum horizontal stress, breakdown may not occur even with high mud weight, Fig. 13-a and b.

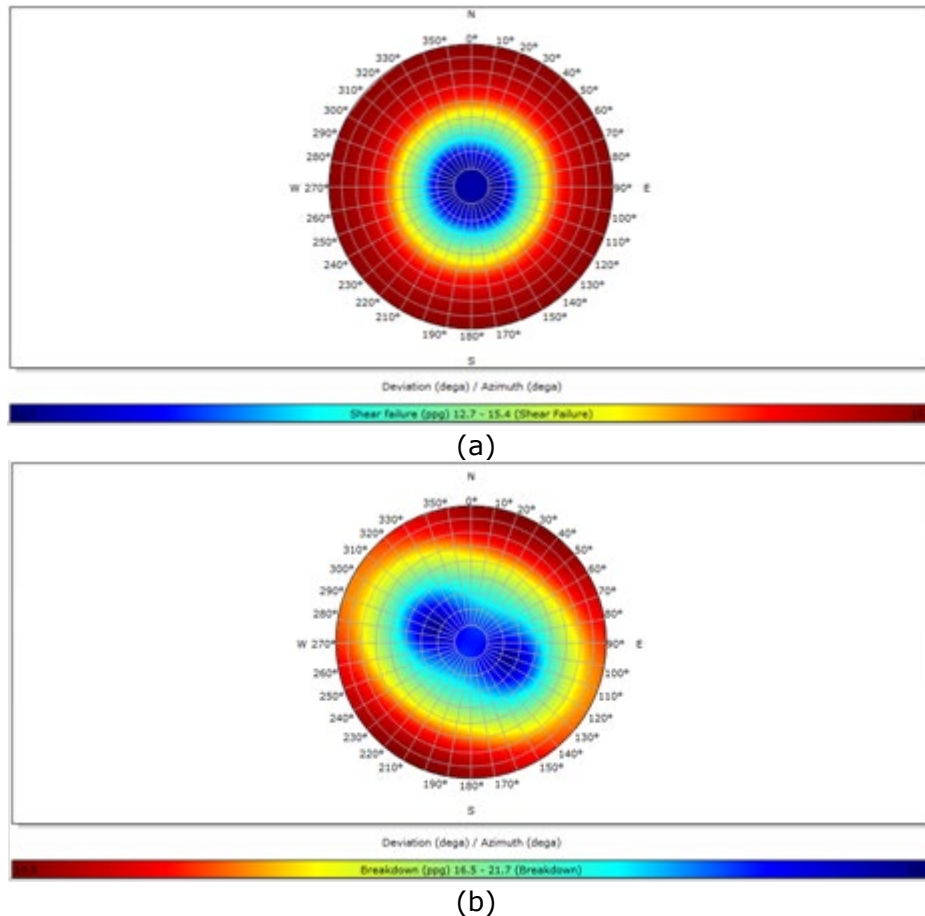


Fig. 13. Plots of mini-mud weight by using Mogi-Coulomb failure criterion: (a) breakout mud weight vs. orientation, (b) breakdown mud weight vs. orientation.

#### 4. Conclusions

To achieve an accurate estimation of rock failure criteria, 1D-MEM constructing is essential step. an integrated data information is required such as well logs (caliper log, bit size, sonic log, gamma ray and bulk density), drilling formation data (daily drilling report, final drilling report, geological report). Depending on far-field stress relation ( $\sigma_v$ ,  $\sigma_H$  and  $\sigma_h$ ), we found that (Mishrif C1, Mishrif C2, Mishrif A, Mishrif B1, Mishrif B2, Mishrif C3, Mauddud, Nahr Umr B, Ahmadi and Zubair) are normal fault and (Nahr Umr A, Shuaiba, Ratawi and Yamama) are Strike-slip fault and Rumaila is Reverse fault. Ultimately, it can be choosing the appropriate and best failure criterion to be used in building a geomechanical model to create drilling programs. This step is crucial for planned wells and to make real-time revisions to those programs has proven valuable in successfully drilling the hazardous intervals while reducing the costs and duration of the planned well delivery. Also, based on the sensitivity analysis. Therefore, for inclinations 60 degrees and above, shear failure occurs even in both directions of minimum and maximum horizontal stress, and stereonet plots for breakdown show that tensile failure most likely occurs with inclination of the well is about 800 and above towards of maximum horizontal stress.

#### References

- [1] Bradley WB. Failure of inclined boreholes. J. Energy Resour. Technol. Trans. ASME, 1979; 101(4): 232-239.
- [2] Plumb RA. Influence of composition and texture on the failure properties of clastic rocks. Soc. Pet. Eng. - Rock Mech. Pet. Eng., 1994; 13-20. <https://doi.org/10.2118/28022-ms>

- [3] Zoback MD, Barton CA, Brudy M, Castillo DA, Finkbeiner T, Grollmund BR Moos, DB, Peska P, Ward CD, Wiprut DJ. Determination of stress orientation and magnitude in deep wells. *International Journal of Rock Mechanics and Mining Sciences*, 2003; 40(7–8): 1049–1076. <https://doi.org/10.1016/j.ijrmms.2003.07.001>.
- [4] Al-Ajmi AM, and Zimmerman RW. Stability analysis of vertical boreholes using the Mogi-Coulomb failure criterion. *Int. J. Rock Mech. Min. Sci.*, 2006; 43(8): 1200–1211. <https://doi.org/10.1016/j.ijrmms.2006.04.001>
- [5] Rasouli. The influence of perturbed stresses near faults on drilling strategy: A case study in Blacktip field, North Australia. *J. Pet. Sci. Eng.*, 2011; 76(1–2): 37–50, 2011. <https://doi.org/10.1016/j.petrol.12.003>
- [6] Al-Kattan W, Al-Ameri NJ. Estimation of the rock mechanical properties using conventional log data in North Rumaila field. *Iraqi Journal of Chem and Pet Eng*, 2012; 13: 27–33.
- [7] Rahimi R. The effect of using different rock failure criteria in wellbore stability analysis. Masters Thesis, p. 72, 2011; [https://scholarsmine.mst.edu/masters\\_theses/7270](https://scholarsmine.mst.edu/masters_theses/7270)
- [8] Mansourizadeh M. Wellbore stability analysis and breakout pressure prediction in vertical and deviated boreholes using failure criteria – A case study, *Journal of Petroleum Science and Engineering*, 2016; 145: 482–492. <https://doi.org/10.1016/j.petrol.2016.06.024>
- [9] Aqrabi AM. Carbonate–siliciclastic sediments of the Upper Cretaceous (Khasib, Tanuma, and Sa'di Formations) of the Mesopotamian Basin. *J. Mar. Pet. Geol.*, 1996; 13(7): 781–790.
- [10] PetroChina report. Field Development Plan Revision No.1 of Halfaya. Internal report, 2018.
- [11] Al-Ameri NJ, Hamd-Allah SM, and Abass H. Evaluation of Geomechanical Properties for Tight Reservoir Using Uniaxial Compressive Test, Ultrasonic Test, and Well Logs Data. *Petroleum and Coal*; 2020; 62(2): 329–340.
- [12] Aadnoy BS, and Limite C. *Petroleum Rock Mechanics: Drilling Operations and Well Design*. 2010; 23(6): 681–694.
- [13] Reynolds SD. Constraining stress magnitudes using petroleum exploration data in the Cooper-Eromanga Basins, Australia, *Tectonophysics*, 2006; 415(1–4): 123–140. <https://doi.org/10.1016/j.tecto.2005.12.005>
- [14] Al-Ameri NJ, Hamd-Allah S, Abass H. Investigating geomechanical considerations on suitable layer selection for hydraulically fractured horizontal wells placement in tight reservoirs. In: Abu Dhabi International Petroleum Exhibition and Conference (ADIPEC), 2020; <https://doi.org/10.2118/SPE-203249-MS>
- [15] Al-Ameri NJ, Hamd-Allah S, Abass H. Specifying Quality of a Tight Oil Reservoir through 3-D Reservoir Modeling. *Iraqi Journal of Science*, 2020; 3252–3265.
- [16] Bell JS. Practical Methods for Estimating in Situ Stresses for Borehole Stability Applications in Sedimentary Basins'. *Journal of Petroleum Science and Engineering* 2003; 38(3–4): 111–19. [https://doi.org/10.1016/S0920-4105\(03\)00025-1](https://doi.org/10.1016/S0920-4105(03)00025-1)
- [17] Richard P. The Mechanical Earth Model Concept and Its Application to High-Risk Well Construction Projects. *Journal of Petroleum Science and Engineering* 2007; <https://doi.org/10.2523/59128-ms>
- [18] Al-Ameri NJ. Laboratory-Based Correlations to Estimate Geomechanical Properties for Carbonate Tight Reservoir. *Petroleum and Coal*, 2022; 64 (4): 804–812.
- [19] Alameedy U. Accurate Petrophysical Interpretation of Carbonate using the Elemental Capture Spectroscopy (ECS). *Iraqi Journal of Chemical and Petroleum Engineering*, 2023; 24(3):
- [20] Zhang J. Borehole Stability Analysis Accounting for Anisotropies in Drilling to Weak Bedding Planes'. *International Journal of Rock Mechanics and Mining Sciences*, 2013; 60: 160–70. <https://doi.org/10.1016/j.ijrmms.2012.12.025>
- [21] Al-Ameri NJ, Hamd-Allah S. Sonic Scanner Helps in Identifying Reservoir Potential and Isotropic Characteristics of Khasib Formation. *Iraqi Geological Journal*, 2023; 56 (1D).
- [22] Al-Ameri NJ. Perforation location optimization through 1-D mechanical earth model for high-pressure deep formations. *Journal of Petroleum Exploration and Production Technology* , 2021; 11 (12): 4243–4252.
- [23] Hamd-Allah SM, Al-Ameri NJ. Investigating tight oil reservoir production performance: Influence of geomechanical parameters and their distribution. *Petroleum Research*, 2023; 8(4): 490–498. <https://doi.org/10.1016/j.ptlrs.2023.05.002>.

To whom correspondence should be addressed: Nagham J. Al-Ameri, Petroleum Engineering Department, College of Engineering, University of Baghdad, Baghdad, Iraq, E-mail: [naghamjasim@coeng.uobaghdad.edu.iq](mailto:naghamjasim@coeng.uobaghdad.edu.iq)